Analytical Model of SIGMA: End-to-End Seamless Mobility Management for Data Networks

Shaojian Fu, **Mohammed Atiquzzaman**, **Harsha Sirisena**

TR-OU-TNRL-07-105
Nov 2007

Telecommunication & Network Research Lab

School of Computer Science

THE UNIVERSITY OF OKLAHOMA

200 Felgar Street, Room 159, Norman, Oklahoma 73019-6151
(405)-325-4042, atiq@ou.edu, www.cs.ou.edu/~atiq

Analytical Model of SIGMA: End-to-End Seamless Mobility Management for Data Networks

Shaojian Fu
OPNET Technologies,
7255 Woodmont Avenue,
Bethesda, MD 20814-7900.

Mohammed Atiquzzaman
School of Computer Science,
University of Oklahoma,
Norman, OK 73019-6151.

Harsha Sirisena
Dept. of Elect. & Computer Engg.,
University of Canterbury,
Christchurch, New Zealand.

***Abstract*—A new end-to-end seamless mobility management protocol, called Seamless IP diversity-based Generalized Mobility Architecture (SIGMA), which utilizes multi-homing to achieve seamless handover of a mobile host and overcomes a number of performance bottlenecks and security limitations of Mobile IP, has been proposed in the literature. Various performance aspects of SIGMA have been widely studied in the literature using simulation and experimental prototype. Simulation and experimental results are, however, specific to the scenario being studied and cannot be used to generalize the performance of SIGMA. In this paper, we propose an analytical model to evaluate the performance of SIGMA for a wide range of mobile host velocities, propagation delay between communicating peers, error rate, and receiver power.**

I. Introduction

Mobile IP (MIP) [1] is an IETF standard to handle mobility of Internet hosts for mobile data communication. It enables a TCP connection to remain alive and receive packets when a mobile host moves from one point of attachment to another. While MIP is a widely accepted concept in both research and industry, several problems exist when using MIP in a mobile computing environment. The most important issues of base MIP identified to date include high handover latency [2], high packet loss rate [3], [4], and conflict with network security solutions [2].

To overcome the performance bottlenecks and security issues of MIP, a new end-to-end mobility management scheme called Seamless IP diversity based Generalized Mobility Architecture (SIGMA) has been proposed in the literature [5], [6]. The basic idea of SIGMA is to exploit multi-homing to keep the old path alive while setting up the new path, thus achieving a seamless handover between adjacent subnets. The performance evaluation of SIGMA has been extensively carried out using simulation and experimental prototype [7]–[11]. However, simulation and experimental prototype does not permit a general performance evaluation of any scheme. In order to generalize the performance of SIGMA, an analytical framework of SIGMA is required. The *objective of this paper is to propose an analytical model for* SIGMA to permit a comprehensive and systematic way to evaluate the performance of SIGMA.

The Stream Control Transmission Protocol [12] is a new transport layer protocol from IETF. It is based on the congestion control principles of TCP but has additional features such as multihoming and multistreaming, where a number of streams between two end points is called an association. We utilize the multihoming feature of SCTP to illustrate SIGMA which requires multiohoming and multiple IP addresses for seamless handoff. As part of our SIGMA model, we first develop an analytical model for SCTP associations between multihomed nodes. During recent years, several papers have reported analytical models to predict the throughput of TCP during *bulk file transfers* [13]–[16]. The models by Lakshman et al. [13] and Mathis et al. [14] only considered slow start and congestion avoidance, but did not take into account timeouts. The model proposed by Padhye et al. [15] improves the one by Mathis et al. [14] by considering the effect of timeouts and limited receiver window; this model is more accurate than previous models for correlated losses and a wide range of packet loss rates. Casetti et al. [16] proposed using fixed-point to model the interaction between the TCP congestion control and network dynamics, which enables investigation of TCP performance under more complicated network scenarios.

TCP does not support multihoming; therefore, none of the above TCP models considered the effect of multihomed node on the steady state throughput of transport protocols. Our SCTP analytical model differs from previous TCP-related models by explicitly taking multihoming into account in the performance analysis of end-to-end associations between two nodes. We use the SCTP model to develop a general analytical model for SIGMA- the main thrust of this paper. The *authors are not aware* of any analytical model for performance evaluation of end-to-end mobility management schemes

using multihomed nodes.

TCP and SCTP share many congestion control algorithms, such as slow start, congestion avoidance, and fast retransmit. It is thus natural to build on existing TCP models to model congestion control for multihomed SCTP nodes. In this paper, we use the fixed-point method [16] to model the performance of SCTP associations over multihomed nodes.

The generalized SIGMA model is split into two part: source model and network model. The network model is again split into three sub-models: queue, wireless, and handover model. The network model uses the output from the source model as the arrival traffic, and the the source model uses the delay/loss distribution output from the network model to compute the new traffic rate to be generated by an SCTP source. This feedback procedure is repeated until the whole system arrives at an equilibrium point. The advantage of this methodology lies in its ability to isolate the analysis of SCTP's congestion control algorithms from network dynamics, thereby making the model accurate and easy to understand.

The *contributions* of this paper are summarized below:

- Proposed an analytical model for throughput evaluation of multihomed SCTP nodes.
- Proposed an analytical model for SIGMA which can used for the performance evaluation of IP diversity-based end-to-end mobility management schemes.
- Provided a mechanism to compare different handover policies in SIGMA.
- Validated the model by comparison with simulation results.

The rest of the paper is organized as follows. First, the modeling approach of the analytical model of SIGMA is described in Sec. II. The detailed model of SCTP source and network sub-models are presented in Secs. III and IV, respectively. We present the numerical results based on our proposed model in Sec. V. Finally, concluding remarks can be found in Sec. VI.

II. Analytical Model Overview

In this section, we describe our overall modeling approach, including the assumptions for developing our model (Sec. II-A) and the main structure of the analytical model (Secs. II-B to II-D). The notations used in the modeling process are listed in Sec. II-E.

We consider the network topology shown in Fig. 1, which is a typical scenario for mobile handover. Here, Correspondent Node (CN) is associated with N FTP flows which send data to the Mobile Host (MH); AR1 and AR2 are two access routers, through which MH can connect to the network. (B_1, K_1) through (B_5, K_5) are bandwidths and queue sizes of the links in the topology.

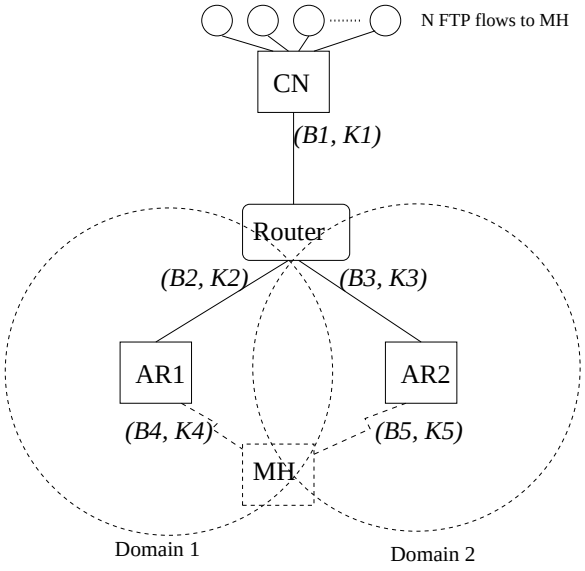

Fig. 1. Network topology.

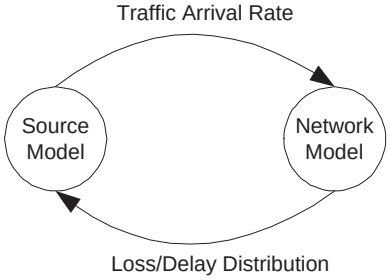

Fig. 2. Overall modeling architecture.

A. Modelling Assumptions

For developing are analytical model we make the following assumptions, which are generally accepted in the literature [16]–[18].

- By considering a large number of SCTP sources, the aggregated traffic into the network can be regarded as a Poisson arrival;
- Loss between subsequent segments in the network are independent;
- Round Trip Time (RTT) has an exponential distribution.

B. Overall architecture

The overall modeling architecture is shown in Fig. 2. The output from the source model is fed into the network model as the arrival traffic, and the output from the network model is fed back into the source model to compute the new arrival traffic pattern. This process is iterated until subsequent iterations generate similar results, representing an equilibrium point for the model.

In the networking scenario shown in Fig. 1, packet losses may happen due to queue overflow at the link

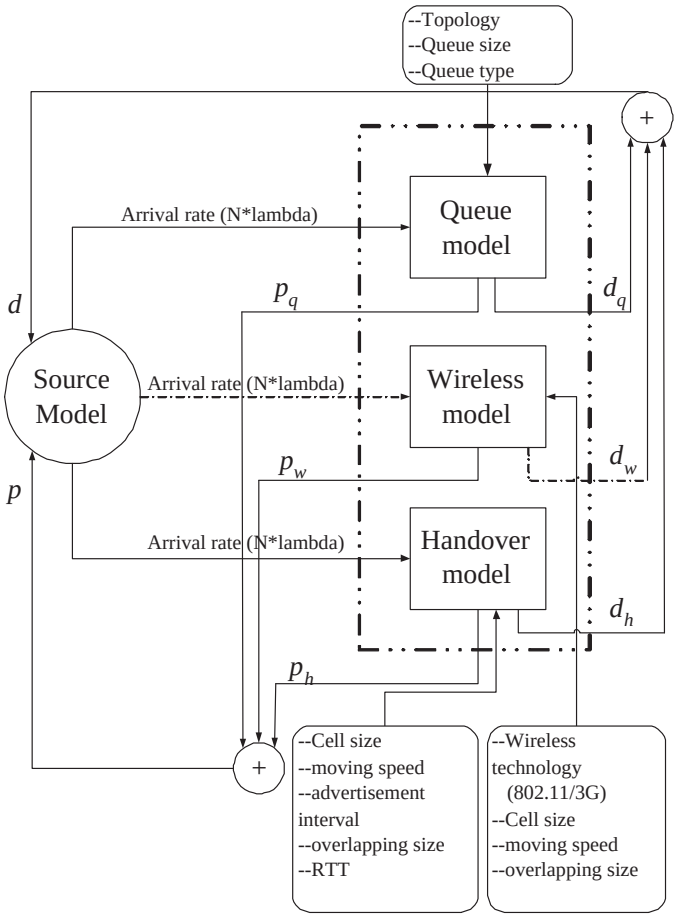

Fig. 3. Detailed Source model - Network model feedback architecture.

queues, wireless link corruption error, or mobile handovers. Data packets may also go through extra delay due to queuing, wireless media contention, or handover latency. According to the type of reasons that contribute to packet losses and delays, we further divide the Network Model in Fig. 2 into three sub-models: *Queue model*, *Wireless model* and *Handover model*, which will be discussed in detail in Sec. II-C. The traffic generated from Source model is fed into the sub-models, and the packet loss rate and delay obtained from separate sub-models are combined and fed back to the Source model.

C. Details of interaction between Source Model and Network Sub-models

The detailed feedback between Source Model and Network Sub-models is shown in Fig. 3. The function and inputs/outputs of the sub-models are described below:

- ***Source model***: The Source model captures the dynamics of SCTP congestion control.
  Inputs: Packet loss probability (combination of p_q, p_w, p_h) and packet delay (combination of d_q, d_w, d_h) which are obtained from the outputs of the Queue model, Wireless model, and Handover model.
  Outputs: The number of SCTP sources (N) and the average arrival rate of individual SCTP sources (λ); these are fed into Queue model, Wireless model, and Handover model.
- ***Queue model***: Queue model captures the packet loss and delay caused by queue waiting and overflow.
  Inputs: In addition to the traffic rate from the Source model, the input includes network topology, queue size, service rate, and queue type.
  Outputs: Packet loss probability and packet delay(p_q, d_q).
- ***Wireless model***: Wireless model captures wireless link corruption errors and packet losses due to user's mobility.
  Inputs: In addition to feeding the output from the source model, the input includes the wireless technology (802.11/ 3G), cell size, moving speed of mobile host, and overlapping size between cells.
  Outputs: Packet loss probability and packet delay (p_w, d_w).
  The link connecting Source model and Wireless model is a dashed line representing uncertainty at this time whether the loss and delay of Wireless model is dependent on the input traffic (one possibility is the increased collision due to MAC layer). Also, the delay output of the Wireless model (d_2) is a dashed line because extra delay introduced by the Wireless model is currently not considered.
- ***Handover model***: Handover model captures the packet loss and delay in case the MH cannot update CN fast enough after it receives advertisement from the new domain.
  Inputs: In addition to traffic rate from the Source model, the input includes cell size, moving speed, advertisement interval, overlapping size, and RTT.
  Outputs: Packet loss probability and packet delay(p_h, d_h).

D. Convergence of the feedback between Source model and Network model

After we obtain the value of packet loss probability (p) and delay, they are fed back into the source model to compute the newly generated traffic rate (λ_{source}). This traffic will then become the input traffic to the network model to recompute a new set of p and d. This process is iterated until the traffic rate (λ_{source}) generated from the previous iteration is close enough to the current iteration.

E. Notations

The notations used in this paper are given below.

- p_q, p_w, p_h Segment loss probability from the output of Queue model, Wireless model, and Handover model, respectively.
- p Combined loss probability from p_q, p_w, p_h.
- d_q, d_w, d_h Mean delay output from Queue model, Wireless model, and Handover model, respectively.
- d Combined delay from d_q, d_w, d_h.
- d_{prop} Propagation delay between source and destination.
- θ Round Trip Time (RTT) between source and destination, which is equal to $d_{prop} + d$.
- $cwnd$ Congestion window size.
- W_t Slow start threshold.
- $wmax$ Maximum value of $cwnd$.
- l Loss indication.
- N Number of SCTP sources.
- T Retransmission Time Out value (RTO).
- $ccwnd$ $cwnd$ size after a state transition.
- $pcwnd$ $cwnd$ size before a state transition.
- Q Transition probability matrix of Markov chain.
- π Steady state distribution of tuple ($cwnd$, W_t, l).
- $P_w(j)$ Probability of j segments lost in a window of size w.
- P_w^{TO} Probability that a Time Out (TO) occurred when $cwnd$ was w.
- P_w^{FR} Probability that a Fast Retransmit (FR) occurred when the $cwnd$ was w.
- $P\left(loss^{(k)}\right)$ Probability that k segments were lost during the last state transition.
- $P\left(pcwnd^{(i)}, ccwnd^{(j)}\right)$ Probability that $pcwnd = i$ and $ccwnd = j$.
- $P\left(pcwnd^{(i)}, ccwnd^{(j)} | loss^{(k)}\right)$ Given k segments were lost during last state transition, probability that $pcwnd = i$ and $ccwnd = j$.
- $P\left(loss^{(k)} | pcwnd^{(i)}, ccwnd^{(j)}\right)$ Given $pcwnd = i$ and $ccwnd = j$, probability that k segments were lost during the last state transition.
- $E\left(L | ccwnd^{(w)}\right)$ Conditional expectation of segment losses occurring in the last transition.
- G Expected number of total segments generated by source model per RTT.
- $E(L)$ Expected number of total losses per RTT.
- λ_{source} Traffic rate generated by source model (Segments/sec).
- λ Arrival traffic rate for a link queue (Segments/sec).
- μ Link service rate (Segments/sec).
- B Link bandwidth (bps)
- K Link queue size (segments).

III. SCTP SOURCE MODEL

In this section, we develop the average traffic rate generated by a SCTP source depending on an input of packet loss probability p and packet delay d. We first consider a single-homed SCTP association case then a multihomed association case.

A. SCTP Congestion Control Overview

SCTP congestion control is based on the well proven rate-adaptive window-based congestion control scheme of TCP. This ensures that SCTP will reduce its sending rate during network congestion and prevent congestion collapse in a shared network. Similar to TCP, the congestion control mechanisms of SCTP include: Slow Start, Congestion Avoidance, Timeout, and Fast Retransmit [19].

However, there are also several major differences between TCP and SCTP congestion control as listed below:

- SCTP doesn't have an explicit fast-recovery phase. SCTP achieves fast recovery automatically with the use of SACK [19].
- The use of SACK is mandatory in SCTP, which allows more robust reaction in the case of multiple losses from a single window of data. This avoids a time-consuming slow start stage after multiple segment losses, thus saving bandwidth and increasing throughput.
- TCP begins fast retransmission after the receipt of three DupACKs; SCTP begins after four DupACKs. SCTP is able to clock out new data on receipt of the first three DupACKs and retransmit a lost segment by ignoring whether the flight size is less than *cwnd*; TCP can only begin data retransmission on the receipt of the third DupACK.

B. Single-homed SCTP Association

We show the state transition diagram of an SCTP association with one destination in Fig. 4, It is based on TCP's state transition diagram [16] but incorporates two differences between TCP and SCTP: (a) SCTP's slow start begins with two segments instead of one, (b) SCTP begins fast retransmit after receipt of four DupACKs, and therefore, the triggering of fast retransmit in SCTP requires a current congestion window of at least five, whereas it is four for TCP.

In Fig. 4, every state includes three elements ($cwnd$, W_t, l), where l is the loss indication: 0 means no loss

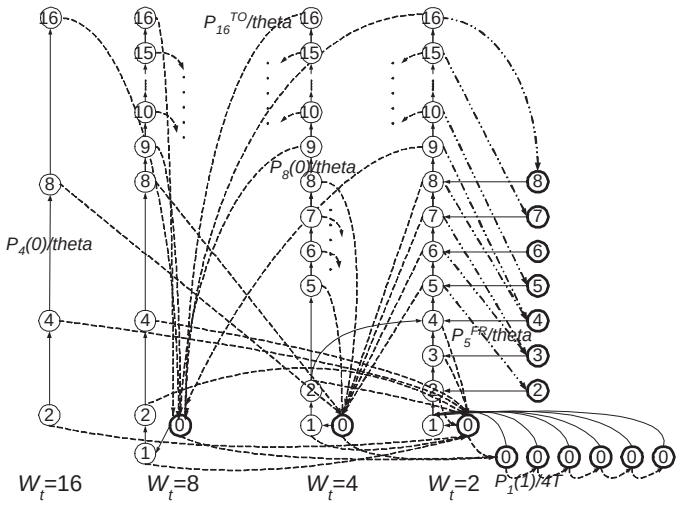

Fig. 4. State transition of SCTP source - single-homed case.

occurred during previous transition and 1 means one or multiple losses occurred. For ease of reading, only $cwnd$ is shown in the circles, and thick circles correspond to states with $l = 1$. Here, $wmax = 16$ is assumed to model the largest receiver window ($rwnd$) of 16, and initial $W_t = wmax$. The rightmost column with thick circles denotes states undergoing fast retransmission. Since this column is identical for $W_t = 2, 4, 8, 16$, for ease of readability, only the case for $W_t = 2$ is shown.

The state transitions in Fig. 4 can be classified into four categories:

- ***Slow Start***: State transitions from (w, W_t, 0) to ($2w$, W_t, 0) with a transition rate of $P_w(0)/\theta$. This means sender's congestion window size grows from w to $2w$ in one RTT, if there is no loss. For example, in Fig. 4, the transition probability from $cwnd = 4$ to 8 at $W_t = 16$ is $P_4(0)/\theta$.
- ***Congestion Avoidance***: State transitions from (w, W_t, 0) to ($w + 1$, W_t, 0) with transition rate of $P_w(0)/\theta$. This means sender's current window size grows from w to $w + 1$ in one RTT, if there is no loss. For example, in Fig. 4, the transition probability from $cwnd = 8$ to 9 at $W_t = 4$ is $P_8(0)/\theta$.
- ***Timeout***: State transitions from (w, W_t, 0) to (0, $\lfloor w/2 \rfloor$, 1) with transition rate of P_w^{TO}/θ. This means sender's current window size drops from w to 0, and slow start threshold drops from W_t to $\lfloor w/2 \rfloor$, and l changes from 0 to 1 within one RTT, if timeout happens.

$$P_w^{TO} = \begin{cases} \sum_{i=1}^{w-4} P_w(i)\left(1-(1-p_q)^i\right) + \sum_{i=w-3}^{w} P_w(i) & w \geq 5 \\ 1 - P_w(0) & w < 5 \end{cases} \quad (1)$$

Although $cwnd = 1$ after a timeout in SCTP, we add the state $cwnd = 0$ as an intermediate state to model the waiting time before a timeout is detected. During this time, no segment is sent, so we count $cwnd$ as 0. For example, in Fig. 4, the transition probability from ($cwnd = 16$, $W_t = 4$, 0) to ($cwnd = 0$, $W_t = 8$, 1) is P_{16}^{TO}/θ.

- ***Exponential Backoff***: In case of repeated timeouts, the SCTP sender will perform an exponential backoff. State transitions from (0, W_t, 1) to (0, 2, 1) with transition rate of $P_1(1)/(2^j T)$, $j = 1, 2, \cdots, 6$ for jth successive timeout. An example in Fig. 4 is the transition rate from the second to third timeout is $P_1(1)/4T$.
- ***Fast Retransmit***: State transitions from (w, W_t, 0) to ($\lfloor w/2 \rfloor$, $\lfloor w/2 \rfloor$, 1) with transition rate of P_w^{FR}/θ. This means that sender's $cwnd$ drops from w to $\lfloor w/2 \rfloor$, slow start threshold drops from W_t to $W_t/2$, and l changes from 0 to 1 in one RTT if timeout happens.

$$P_w^{FR} = \begin{cases} 1 - P_w^{TO} - P_w(0) & w \geq 5 \\ 0 & w < 5 \end{cases} \quad (2)$$

For example, in Fig. 4, the transition rate from ($cwnd = 5$, $W_t = 2$, 0) to ($cwnd = 2$, $W_t = 2$, 1) is P_5^{FR}/θ.

If we assume packet losses to be independent from each other, $P_w(j)$ in Eqns. (1) and (2) can be determined by the Bernoulli formula: $P_w(j) = \binom{j}{w} p_q^j (1-p_q)^{(w-j)}$.

After all transition rates in Fig. 4 are determined, the steady state distribution (π) of ($cwnd$, W_t, l) can be calculated by:

$$\pi Q = \pi \quad (3)$$

where, Q is the transition probability matrix.

C. Multihomed SCTP association

We denote the expected number of segments generated by the source model per RTT as:

$$G = \sum_{w=1}^{wmax} wP\left(cwnd^{(w)}\right) \quad (4)$$

By definition of π,

$$P\left(cwnd^{(w)}\right) = \sum_{W_t=2}^{wmax} \sum_{l=0}^{1} \pi(w, W_t, l) \quad (5)$$

To model an SCTP association with a multihomed destination, we next determine the traffic sent into the primary and alternative paths. We need to model SCTP's packet retransmission on the alternative path when there is a Time Out (TO) or a Fast Retransmit (FR). To do this, in Fig. 4, we strip the states with $l = 1$, and sum up all the losses when the system transits into these states (resulted from TO or FR) to obtain the total number of packets retransmitted on the alternative path, as shown in Fig. 5.

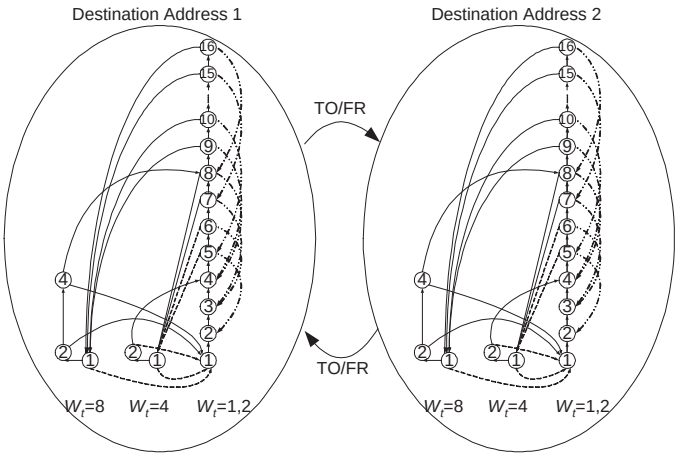

Fig. 5. State transition of SCTP source - multihomed case.

Bayes method is used to compute the expected number of segment losses during these types of transitions as described in detail in Sec. III-D.

D. Bayes Loss Estimation

1) When the transition to the current state with $cwnd = w$ is due to a Fast Retransmit and $ccwnd = w$, then previous window size $pcwnd$ must be $2w$ or $2w+1$. From Fig. 4, the $ccwnd$ can only range from 2 to $wmax/2$ after a Fast Retransmit, and the number of losses during this transition can not be more than $2w-4$; otherwise a timeout will occur. From Bayes formula:

$$\frac{P\left(loss^{(k)}|pcwnd^{(i)},ccwnd^{(w)}\right)=}{\frac{P\left(loss^{(k)}\right)P\left(pcwnd^{(i)},ccwnd^{(w)}|loss^{(k)}\right)}{P\left(pcwnd^{(i)},ccwnd^{(w)}\right)}} \quad \text{where } 2\le w\le wmax/2, i=2w \text{ or } 2w+1 \text{ and } 1\le k\le 2w-4 \tag{6}$$

Since we know that $P\left(loss^{(k)}\right) = P_i(k)$ and $P\left(pcwnd^{(i)},ccwnd^{(w)}\right) = P_i^{FR}$, Eqn. (6) becomes:

$$\frac{P\left(loss^{(k)}|pcwnd^{(i)},ccwnd^{(w)}\right)=}{\frac{P_i(k)P\left(pcwnd^{(i)},ccwnd^{(w)}|loss^{(k)}\right)}{P_i^{FR}}} \tag{7}$$

Next, we want to find $P\left(pcwnd^{(i)},ccwnd^{(w)}|loss^{(k)}\right)$ in Eqn. (7). Since the transition to the current state is caused by a Fast Retransmit, given k segments lost from original transmission, $ccwnd$ will become w only when all the successive retransmissions for the k segments are successful. A timeout will happen if any of the k retransmissions are lost. So, the conditional probability that $pcwnd$ was i and $ccwnd$ becomes w, given k losses happen, can be estimated as:

$$P\left(pcwnd^{(i)},ccwnd^{(w)}|loss^{(k)}\right)=(1-p)^k \tag{8}$$

By substituting Eqn. (8) into Eqn. (7), we get:

$$P(loss^{(k)}|pcwnd^{(i)},ccwnd^{(w)})=\frac{P_i\left(k\right)\left(1-p\right)^k}{P_i^{FR}} \tag{9}$$

By summing up two cases for $i=2w,2w+1$ in Eqn. (9), we get the marginal conditional distribution:

$$P(loss^{(k)}|ccwnd^{(w)})=\sum_{i=2w}^{2w+1}\frac{P_i\left(k\right)\left(1-p\right)^k}{P_i^{FR}} \tag{10}$$

2) When the transition to the current state resulted from a timeout, then $ccwnd$=0, and $pcwnd$ could be any value from 1 to $wmax$, and $k = 1,2,\ldots pcwnd$. Similarly, by Bayes Formula:

$$\frac{P\left(loss^{(k)}|pcwnd^{(w)},ccwnd^{(0)}\right)=}{\frac{P\left(loss^{(k)}\right)P\left(pcwnd^{(w)},ccwnd^{(0)}|loss^{(k)}\right)}{P\left(pcwnd^{(w)},ccwnd^{(0)}\right)}} \tag{11}$$

Since we know that $P\left(loss^{(k)}\right) = P_w(k)$ and $P\left(pcwnd^{(w)},ccwnd^{(0)}\right) = P_w^{TO}$, Eqn. (11) becomes:

$$\frac{P\left(loss^{(k)}|pcwnd^{(w)},ccwnd^{(0)}\right)=}{\frac{P_w(k)P\left(pcwnd^{(w)},ccwnd^{(0)}|loss^{(k)}\right)}{P_w^{TO}}} \tag{12}$$

Next, we want to find $P\left(pcwnd^{(w)},ccwnd^{(0)}|loss^{(k)}\right)$ in Eqn. (12). Since the transition to the current state is caused by a timeout, given k segments were lost in the original transmission, if some of the retransmitted segments for the k segments failed or there are not enough DupACK generated (in the case of $k = w-3,w-2,\ldots w$), $ccwnd$ will become zero; otherwise, a Fast Retransmit will happen. Also, because $pcwnd$ can be any value from 1 to $wmax$, we assume that $pcwnd$ ranges from 1 to $wmax$ with equal probability. So, the conditional probability that $pcwnd$ was w, $cwnd$ is 0, given k losses happen, can be estimated as:

$$P\left(pcwnd^{(w)},ccwnd^{(0)}|loss^{(k)}\right)= \begin{cases} \left[1-(1-p)^k\right]/wmax & k=1,2,\ldots w-4 \\ 1/wmax & k=w-3,w-2,\ldots w \end{cases} \tag{13}$$

Substituting Eqn. (13) into Eqn. (12), and by summing up all the cases for $pcwnd = 1,2,\ldots,wmax$, we can get the marginal condi-

tional distribution:

$$P\left(loss^{(k)}|ccwnd^{(0)}\right) = \sum_{pcwnd=1}^{wmax} P\left(loss^{(k)}|pcwnd^{(w)}, ccwnd^{(0)}\right)$$

$$= \begin{cases} \sum_{w=1}^{wmax} \frac{P_w(k)\left[1-(1-p)^k\right]}{wmax P_w^{TO}} & \text{if } k = 1, 2, \ldots w-4 \\ \sum_{w=1}^{wmax} \frac{P_w(k)}{wmax P_w^{TO}} & \text{if } k = w-3, w-2, \ldots w \end{cases} \quad (14)$$

Our next step is to find the expected number of losses given $ccwnd = w$. This is done by weighting the number of segment losses (k) by the conditional probabilities (Eqns. (10) and (14)):

$$E\left(L|ccwnd = w\right) = \sum_{k=1}^{wmax} kP\left(loss^{(k)}|ccwnd^{(w)}\right) \quad (15)$$

Finally, the overall expected segment losses occurring in the primary path, i.e. the traffic transferred into the backup path can be obtained using:

$$E(L) = \sum_{w=1}^{wmax} E\left(L|ccwnd = w\right) P(ccwnd = w)$$
$$= \sum_{k=1}^{wmax} kP\left(loss^{(k)}|ccwnd^{(w)}\right) P(ccwnd = w) \quad (16)$$

The above equation also represents the conditional expectation of segment losses occurring during transiting into the states with $l = 1$. We can thereby obtain the traffic on the primary path by subtracting the losses (Eqn. (16)) from the total traffic generated by the source (Eqn. (4)). Eqn. (16) gives the traffic on the alternative path.

IV. Network sub-models

Solution of the source model in Sec. III requires the value of RTT ($\theta = d_{prop} + d$) and loss probability (p). In this section, we derive the values of d and p by divided each of them into three components related to queueing, wireless fading, and mobile handover, as shown in Fig. 3. Each of these components will be dealt with in the following subsections.

A. Queue model

We consider two cases in the Queue model: single queue and multi-queues. In single queue case, the whole network is modelled as one M/M/1/K queue. In the multi-queue case, we consider the queues in the network separately.

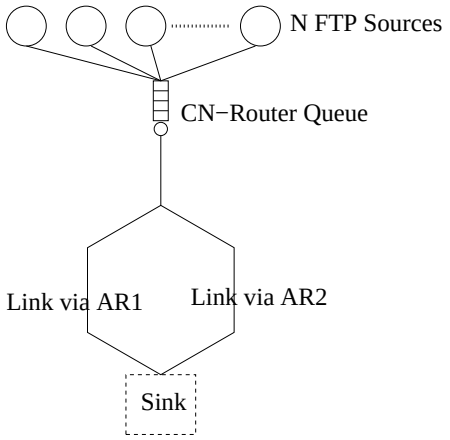

Fig. 6. Queuing network for single queue case.

1) Single queue case: In Fig. 1, when B_2 through B_5 are large enough, the only queue having effect on packet loss and delay is the CN-Router queue. We can model the queuing network as an M/M/1/K queue ($K = K1$), as shown in Fig. 6. We denote $\rho = \frac{\lambda}{\mu}$, where λ is the traffic generated by the Source Model, and $\mu = B/8 * PacketSize$ (segments/sec). From M/M/1/K queuing theory, the segment loss probability can be calculated as:

$$p_q = \begin{cases} \frac{1}{K+1} & \rho \geq 1 \\ \frac{(1-\rho)\rho^B}{1-\rho^{(K+1)}} & \rho < 1 \end{cases} \quad (17)$$

To find the queuing delay (d_q), let's denote S as the mean number of segments in the queue:

$$S = \begin{cases} \frac{K}{2} & \rho = 1 \\ \frac{\rho}{(1-\rho)} - \frac{K+1}{1-\rho^{(K+1)}}\rho^{K+1} & \rho \neq 1 \end{cases} \quad (18)$$

Considering the current segment being transmitted in the queue, we can obtain the mean queuing delay as:

$$d_q = \frac{S+1}{\mu} \quad (19)$$

2) Multi-queue case: In the presence of greedy connections (such as FTP) that tend to overload the network, different queueing models provide similar estimates of the average loss probability [20]. Therefore, a simple queue for each link can be used to approximate the ensemble behavior the whole network. Results of testing other approaches with significantly greater complexity (mainly based on group arrivals and services) did not show a significantly change in the case of long-lived flows [20]. In Fig. 1, if (B_2, K_2) through (B_5, K_5) are finite, we assume the queuing network can be modelled as a combination of M/M/1 queues [20], as shown in Fig. 7. The input traffic to each queue in Fig. 7 can be determined as: $\lambda_{CN-Router} = \lambda_{source}$. This means the input traffic to the CN-Router queue is the same as the

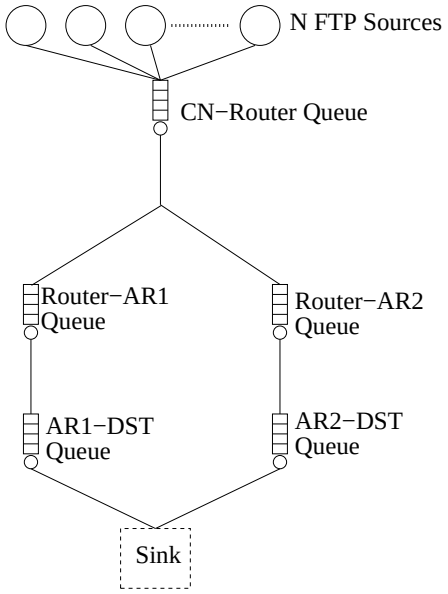

Fig. 7. Queuing network for multi-queue case.

traffic generated from the source model. We can also get the input traffic to the Router-AR1 queue as:

$$\lambda_{Router-AR1} = \lambda_{CN-Router}(1-R)(1-P_{CN-Router})$$

where, $P_{CN-Router}$ denoting the loss probability at CN-Router queue can be determined using Eqn. (17) with $\lambda = \lambda_{CN-Router}$, $B = B1$, and $K = K1$. R is the percentage of packets retransmitted through the alternative path (via AR2), which can be determined as:

$$R = E(L)/G$$

where, $E(L)$ is the expected number of packet losses during one RTT (as determined by Eqn. (16), which will be retransmitted through the alternative path), and G (determined by Eqn. (4)) is the total traffic generated by the source model. Similarly, we can get the input traffic to the AR1-MH queue:

$$\lambda_{AR1-MH} = \lambda_{Router-AR1}(1-P_{Router-AR1})$$

Since each queue is modelled as an M/M/1/K queue, we can use Eqns. (17) and (18) to obtain the loss probability and average queue occupancy of each individual queue. Assuming no loss in the alternative path, we can get the overall loss probability at the primary path as:

$$p_q = 1-(1-P_{CN-Router})(1-P_{Router-AR1})(1-P_{AR1-MH}) \quad (20)$$

where, $P_{Router-AR1}$ and P_{AR1-MH} denote the loss probability at Router-AR1 queue and AR1-MH queue, respectively. This means that the overall loss probability is the percentage of packets that did not go through all these three queues successfully.

Using Little's law, we can model the average delay in the queuing network as:

$$\begin{aligned} d_q &= \frac{S}{\lambda} \\ &= \frac{S_{CN-Router} + S_{Router-AR1} + S_{AR1-MH}}{\lambda} \end{aligned} \quad (21)$$

where, $S_{CN-Router}$, $S_{Router-AR1}$, and S_{AR1-MH} denote the average queue occupancy at CN-Router queue, Router-AR1 queue, and AR1-MH queue, respectively; λ is the input traffic rate at CN-Router queue.

B. Wireless Model

Over the past 30 years, many wireless propagation models have been proposed for wireless link budget design, the most frequently used one being the *Free-space*, *Two-ray ground*, and *Log-normal shadowing* models [21]. The Free-space model and the Two-ray ground model predict the received power as a deterministic function of distance. In reality, the received power at a certain distance is a random variable due to the effect of environment shadowing, which may cause the received power at two different locations having the same transmitter-receiver distance. Consequently, the more general and widely-applicable Log-normal shadowing model (or shadowing model for short) will be used in this paper.

The shadowing model calculates the received power at a receiver at a distance d from transmitter can be calculated by [21]:

$$P_r(d)[dBm] = P_t[dBm] - PL(d)[dB] \quad (22)$$

where, $P_r(d)$ is the received power at distance d from transmitter. $PL(d)$ is called path loss at distance d, which in turn can be calculated by:

$$PL(d)[dB] = \overline{PL(d)} + X_\delta = \overline{PL(d_0)} + 10n\log\left(\frac{d}{d_0}\right) + X_\delta \quad (23)$$

where, X_δ is a zero-mean Gaussian distributed random variable in dB with standard deviation δ (also in dB). d_0 is a reference point in the line-of-sight to the transmitter and where the received signal strength can be precisely measured. n is called path loss exponent, which normally ranges from 4 to 6 for obstructed indoor environments. δ can be computed from measured data, with four being commonly used for simulation and analysis.

The shadowing model can be used to determine the probability of the received signal strength being smaller than a given receiving threshold. Let γ be the receiving threshold, then:

$$P_w = P[P_r(d) < \gamma] = Q\left(\frac{\overline{P_r(d)} - \gamma}{\delta}\right) \quad (24)$$

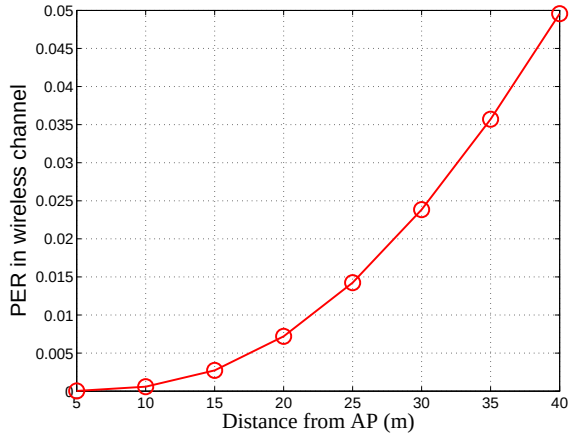

Fig. 8. Packet error rate as a function of distance.

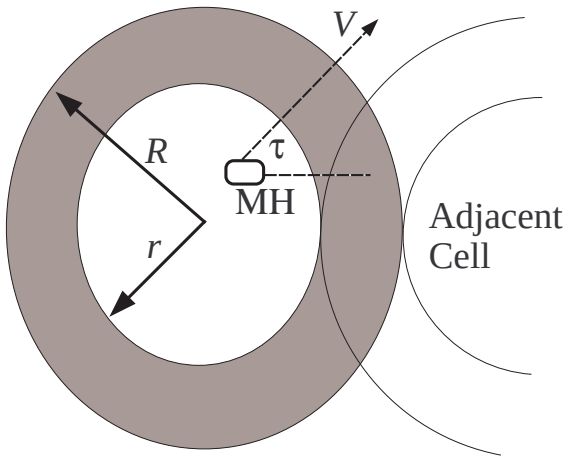

Fig. 9. A cell and its adjacent cell with a mobile host.

where, Q function is defined as:

$$Q(z) = \frac{1}{\sqrt{2\pi}} \int_z^\infty \exp\left(-\frac{x^2}{2}\right) dx$$

A packet transmitted over a wireless link generally goes through source coding, channel coding, spectrum spreading, modulation, and beam-forming procedures to reduce the packet error rate. In this paper, we take a similar approach as in network simulator *ns*-2 [22], and do not consider the effects of these mechanisms to simplify the expression of the model.

We performed some testing in our testbed to characterize the packet error rate generated by the shadowing model. We choose $d_0 = 5\text{m}$ and measured $\overline{Pr(d_0)} \approx -40\text{dBm}$. If threshold γ was selected as -131.5dBm, such that the PER at cell edge is 0.05. With $n = 6$ and $\delta = 4$, we can plot PER in wireless channel P_w as shown in Fig. 8.

C. Handover Model

In this section, the handover model is developed to capture the packet loss rate resulting from SIGMA handover. The cell structure in our model is shown in Fig. 9. It is assumed that every cell is surrounded in all directions by other cells, identical in radio coverage, and due to symmetry, the overlap region is a perfect annulus. The base station is situated at the center of the cell. The shaded area within the cell refers to center coverage, while the unshaded area refers to border coverage.

1) Notations for Handover Model: The notations used in the handover model are listed below:

- V_{max} Maximum velocity of MH.
- V Velocity of MH, uniformly distributed between $[0, V_{max}]$ m/s.
- V_{ref} Maximum velocity for the experiment used to generate curves.
- τ The direction of MH measured from the horizontal, uniformly distributed between $[0, 2\pi]$.
- RTT Round trip time between MH and CN in seconds.
- RTT_{ref} Reference RTT.
- R Radius of wireless cell in meters.
- r Radius of center coverage area in meters.
- G_{ref} Reference overlap region size.
- P_{wb} Wireless channel loss rate when MH is in border coverage.
- θ Minimum time taken to cross overlap region, shortest distance at V_{max}.
- P_c Probability of MH leaving the center coverage.
- P_{ch} Conditional handover packet loss probability given MH leaving the center coverage.
- T_r Subnet residence time.

2) Probability of Mobiles Leaving the Center Coverage: The probability, P_c, of MH crossing the boundary of the center coverage and entering the border coverage region within one RTT was determined using a Monte-Carlo simulation. P_c was obtained for different V_{max}, RTT and r combinations and the resulting curves were accurately fitted to the equations below. Eqn. (25) is the probability obtained for a fixed r of 30 meters, generalized for different values of RTT and V_{max} and RTT_{ref} of 100ms. After varying the value of r, the coefficient α in Eqn. (25) has been expanded to be a function of r. The curve fitting was done using the curve fitting tool in Matlab.

$$\begin{aligned} P_c &= \alpha \frac{RTT}{RTT_{ref}} V_{max} \\ \text{where } \alpha &= 0.00717\text{e}^{-0.1445r} + 0.0018\text{e}^{-0.021r} \end{aligned} \quad (25)$$

3) Conditional Packet Loss Probability During Handover: In this section, we compute the conditional prob-

ability, P_{ch} that a mobile node experiences a packet loss, given it entered the overlap region and continued on its current course until it moved to the adjacent cell. When a MH moves out of the coverage area of the current wireless cell and enters an adjacent cell, it needs to signal CN to add new IP address into the association and set the new IP as the primary destination. If this action, including the RTT, takes more time than the time for the mobile to travel from its current position to the area covered only by the new wireless cell, packets will be sent to an outdated access point resulting in packet loss. Clearly, packet loss probability depends on the mobile speed V and the RTT between the MH and CN.

We used Monte-Carlo simulation to generate samples of mobile users within the center coverage with random coordinates, directions of travel and velocities (V). Users who leave the center coverage and cross into the border coverage within the next RTT are considered. Fig. 10 plots the histogram of the time taken by these users to completely cross the border coverage, t_{cross}, making the simplifying assumption that their velocities remain constant until the crossing is completed.

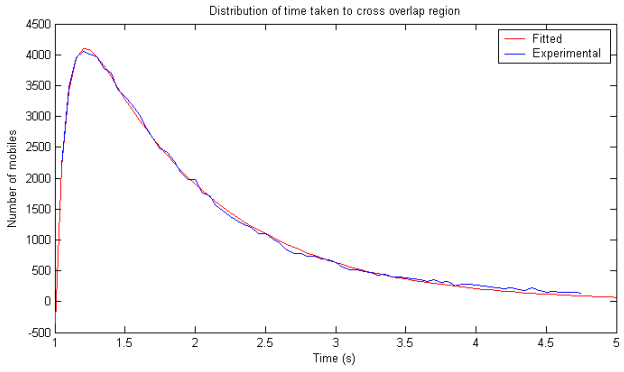

Fig. 10. Distribution of time taken to cross overlap region.

The histogram plot was fitted into a double exponential function given by Eqn. (26). As seen from the Eqn. (26), the fitted function is shifted to the right by θ, which is the time (minimum) needed to cross the overlap region if traversing the shortest distance at a maximum speed. The fitted function was also plotted in Fig. 10. Assuming a Poisson distribution of mobile arrivals and the above stated distributions for positions, velocities and angles we would expect the two exponentials to give a really good fit of the empirical (Monte-Carlo) data.

$$f(t) = \begin{cases} 0 & t < \theta \\ a\mathrm{e}^{b(t-\theta)} - c\mathrm{e}^{d(t-\theta)} & t \geq \theta \end{cases} \tag{26}$$

In Eqn. (26), $\theta = (R-r)/V_{max}$, and a, b, c, d are defined using a common variable K, which is defined as

$$K = \frac{V}{V_{ref}} \left(\frac{R-r}{G_{ref}} \right)^{-1} \tag{27}$$

The curve fitting determined the values of a, b, c and d as follows: $a = 1.1446K$, $b = -1.1026K$, $c = 1.2134K$, and $d = -12.68K$. The empirical data from one scenario can be generalized to any other radius and maximum velocity by simply noting that boundary crossing rate is directly proportional to maximum mobile speed, assuming the Probability Density Function (PDF) of speeds remains rectangular.

We now assume that the total time required to complete a handoff t_{ho}, is uniformly distributed between [t_{min}, t_{max}]; t_{ho} includes the time to perform Layer 2 handover, obtain new IP address, signaling CN about new IP address, as well as register new IP address as the primary destination. Then in order to successfully complete the handoff without any packet loss, we must have:

$$t_{cross} - t_{ho} > 0 \tag{28}$$

If $g(t)$ is the probability density function of t_{ho}, the convolution of the PDFs of t_{cross} and t_{ho} gives us the PDF of the difference, as given by Eqn. (29). Since the distributions of t_{ho} (uniform) and t_{cross} (given in Eqn. (26)) are not continuous, the convolution gives a piece-wise continuous function.

$$f(t) \otimes g(-t) = \begin{cases} 0 & t < \theta - t_{max} \\ M_1\mathrm{e}^{bt} + M_2\mathrm{e}^{dt} + M_3 & \theta - t_{max} \leq t < \theta - t_{min} \\ K_1\mathrm{e}^{bt} + K_2\mathrm{e}^{dt} & t \geq \theta - t_{min} \end{cases} \tag{29}$$

where, K_1, K_2, K_3, M_1 and M_2 are constants for a given V_{max}, t_{min}, t_{max}, R and r. The values of these constants are as follows:

$$\begin{aligned} K_1 &= \tfrac{a}{b(t_{max}-t_{min})} \left[\mathrm{e}^{b(t_{max}-\theta)} - \mathrm{e}^{b(t_{min}-\theta)} \right] \\ K_2 &= -\tfrac{c}{d(t_{max}-t_{min})} \left[\mathrm{e}^{d(t_{max}-\theta)} - \mathrm{e}^{d(t_{min}-\theta)} \right] \\ M_1 &= \tfrac{a}{b(t_{max}-t_{min})} \mathrm{e}^{b(t_{max}-\theta)} \\ M_2 &= -\tfrac{c}{d(t_{max}-t_{min})} \mathrm{e}^{d(t_{max}-\theta)} \\ M_3 &= \left(\tfrac{c}{d} - \tfrac{a}{b}\right) \tfrac{1}{(t_{max}-t_{min})} \end{aligned} \tag{30}$$

In the curve given by Eqn. (29), the area for $t < 0$ gives the packet loss probability (P_{ho}) during handover for an MH crossing into the overlap region. This is the probability that the handover latency will be more than

$$P_{ho} = \begin{cases} \left.\begin{array}{l} \frac{M_1 e^{b\theta}}{b}\left(e^{-bt_{min}} - e^{-bt_{max}}\right) + \frac{M_2 e^{d\theta}}{d}\left(e^{-dt_{min}} - e^{-dt_{max}}\right) + M_3\left(t_{max} - t_{min}\right) \\ \quad + \frac{K_1}{b}\left(1 - e^{b}\left(\theta - t_{min}\right)\right) + \frac{K_2}{d}\left(1 - e^{d}\left(\theta - t_{min}\right)\right) \end{array}\right\} & \theta < t_{min} \\ \frac{M_1}{b}\left(1 - e^{b}\left(\theta - t_{max}\right)\right) + \frac{M_2}{d}\left(1 - e^{d}\left(\theta - t_{max}\right)\right) - M_3\left(\theta - t_{max}\right) & t_{min} \le \theta < t_{max} \\ 0 & \theta \ge t_{max} \end{cases} \tag{31}$$

the cross over time (the opposite of the condition given in Eqn. (28)). We assume MH will continue traveling without change in direction and velocity until it reaches the cell boundary. Integrating the piece-wise continuous convolution, we obtain the handover packet loss rate as shown in Eqn. (31).

The different formulas in Eqn. (31) correspond to the cases of the cross over time being (i) less than the minimum latency, (ii) in between the minimum and maximum latencies, and (iii) greater than the maximum latency. In the latter case, no packet loss is expected as the MH would have completed handover before the crossing takes place, resulting in zero handover loss probability.

4) Handover Packet Loss Probability: Now that we have obtained P_c and P_{ch} as shown in Eqn. (25) and Eqn. (31), respectively, we can compute the handover packet loss probability P_h for any MH in Eqn. (32), where the ratio of the square of the inner and outer radius values gives the proportion of mobiles within the inner circle.

$$P_h = \frac{r^2}{R^2} P_c P_{ch} \tag{32}$$

As an example, for $G_{ref} = 10$, $R = 40$, $r = 30$, $t_{ho} = [0.5, 0.9]$, the probability of packet loss during handover is given in Fig. 11 for a range of V_{max} and RTT values.

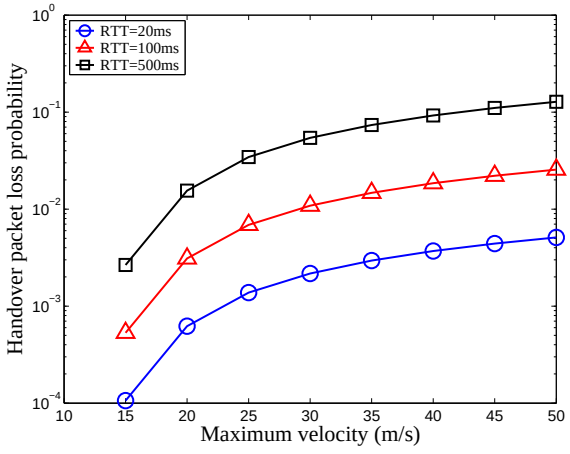

Fig. 11. Handover packet loss probability at various speeds and RTT.

V. Numerical Results

In this section, the source model and three network sub-models (queue model, wireless model, and handover model) are combined according to the feedback structure presented in Sec. II-C. The generated numerical results are presented below. The performance measures used in this section are handover packet loss rate and average end-to-end throughput.

A. Impact of RTT and t_{max}

The impact of RTT and t_{max} on handover packet loss rate is shown in Fig. 12. We can see that with the increase of RTT or t_{max}, the transport layer's end-to-end throughput handover decreases. This is because an increase of RTT means longer time to update CN about the current location of MH, then there is a higher possibility of packets are delivered to an outdated location. plus, for window based transport protocols like SCTP, a higher RTT will limit the rate of pumping data into the network, which will further reduce the end-to-end throughput. Also, a higher t_{max} will produce a higher risk of not finishing handover before MH moves out of overlapping region, which in turn will result in higher packet loss probability and lower throughput.

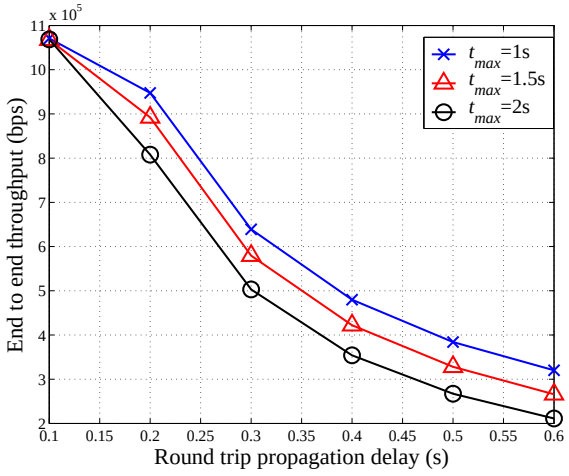

Fig. 12. Impact of RTT and t_{max} on end-to-end throughput.

B. Impact of Moving Speed

The impact of moving speed on the end-to-end throughput under various RTT is shown in Fig. 13. We can see that with the increase of moving speed, the end-to-end throughput decreases due to higher packet loss rate resulting from increased handover frequency. This is because of MH having smaller time to prepare for the handover with higher moving speed. If MH can not receive the ACK for SET_PRIMARY before it moves out of the overlapping region, the packets are delivered to the old location, which causes up to a widow of packets to be lost. As discussed earlier, throughput decreases with increased RTT. However, for $RTT = 20ms$, the throughput remains fairly constant with respect to moving speed. This is because for a small RTT, the time for SIGMA signaling is small enough for the considered moving speeds. Thus, virtually no packet loss happened during handover, and the throughput was not affected.

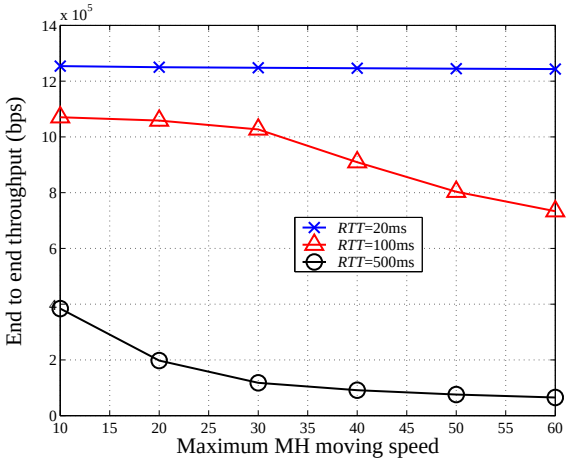

Fig. 13. Impact of moving speed on end-to-end throughput.

C. Impact of Receiver Power Threshold and Cell Size

The impact of receiver power threshold (γ) and cell size (R) on the end-to-end throughput is shown in Fig. 14. We can see that with the increase of γ, the end-to-end throughput decreases resulting from higher packets losses at the receiver side due to receiver power being less than γ. The increase of R has a two-fold impact: (i) It causes the overlapping distance to increase, implying more time for MH to perform SIGMA signaling before it moves out of the old subnet, resulting in decreased packet loss; (ii) A larger cell size implies higher corruption error rate in a wireless channel, which increases the wireless packet loss rate. The results in Fig. 14 show that the wireless packet loss rate dominates, resulting in increase of the overall packet loss rate and decrease of end-to-end throughput with decrease of R.

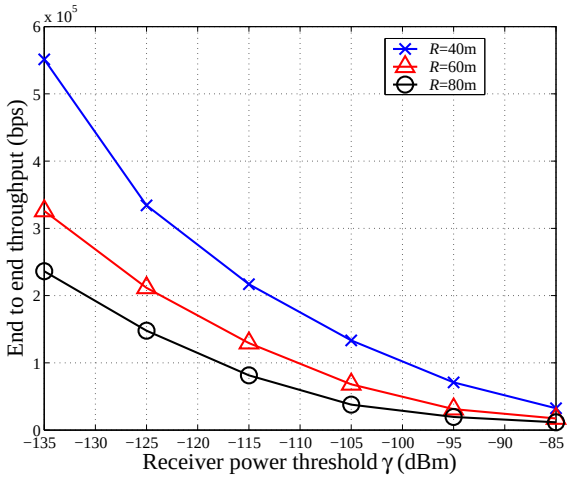

Fig. 14. Impact of receiver power threshold and cell size on end-to-end throughput.

VI. Conclusion

SIGMA is a new end-to-end mobility management protocol which utilizes multi-homing to achieve seamless handover of a mobile host. In this paper, we developed an analytical model to study the performance of SIGMA. The model uses the fixed-point modeling framework, where the output from the source model is fed into the network model, and the output from the network model is fed back to the source model until an equilibrium point is achieved. The network model consists of three sub-models - queue, wireless, and handover models - which form the complete SIGMA model. The sub-models were first developed separately, and subsequently combined to analyze the end-to-end throughput of SIGMA. Using the analytical model, we obtained a better picture of the impact of various parameters on the performance of SIGMA. This modeling methodology can also be generalized to model other similar protocols, such as Mobile IP and its enhancements, by simply modifying the handover model to fit the protocol in question.

References

[1] C.E. Perkins (editor), "IP Mobility Support," IETF RFC 3344, August 2002.

[2] C.E. Perkins, "Mobile Networking Through Mobile IP," *IEEE Internet Computing*, vol. 2, no. 1, pp. 58–69, January/February 1998.

[3] Jarkko Sevanto, Mika Liljeberg, and Kimmo E. E. Raatikainen, "Introducing quality-of-service and traffic classes into wireless mobile networks," in *Proceedings of the 1st ACM International Workshop on Wireless Mobile Multimedia*, Dallas, Texas, 1998, pp. 21–29.

[4] K.E. Malki (editor), "Low latency handoffs in Mobile IPv4," IETF DRAFT, draft-ietf-mobileip-lowlatency-handoffs-v4-07.txt, October 2003.

[5] S. Fu, L. Ma, M. Atiquzzaman, and Y. Lee, "Architecture and performance of SIGMA: A seamless mobility architecture for data networks," in *40th IEEE Internationl Conference on Communications (ICC)*, Seoul, Korea, May 2005.

[6] S. Fu, M. Atiquzzaman, L. Ma, and Y. Lee, "Signaling cost and performance of SIGMA: A seamless handover scheme for data networks," *Journal of Wireless Communications and Mobile Computing*, vol. 5, no. 7, pp. 825–845, Nov 2005.

[7] S. Sivagurunathan, M. Atiquzzaman, and W. Ivancic, "Improving stability of SIGMA handoff," in *IEEE 62nd Semiannual Vehicular Technology Conference*, Dallas, TX, Sep 22-25, 2005, pp. 836–840.

[8] S. Sivagurunathan, J. Jones, M. Atiquzzaman, S. Fu, and Y-J. Lee, "Experimental comparison of handoff performance of SIGMA and mobile IP," in *2005 IEEE Workshop on High Performance Switching and Routing*, Hong Kong, May 12-14, 2005.

[9] S. Fu, M. Atiquzzaman, and W. Ivancic, "Effect of layer 2 handover on SIGMA performance," in *IEEE 62nd Semiannual Vehicular Technology Conference*, Dallas, TX, Sep 25-28, 2005, pp. 2675 – 2679.

[10] S. Fu, M. Atiquzzaman, and W. Ivancic, "Signaling cost evaluation of SIGMA," in *IEEE 62nd Semiannual Vehicular Technology Conference*, Dallas, TX, Sep 25-28, 2005, pp. 2780 – 2784.

[11] S. Fu and M. Atiquzzaman, "Handover latency comparison of SIGMA, FMIPv6, HMIPv6, and FHMIPv6," in *IEEE Globecom*, St. Louis, MO, Nov 28 - Dec 2 2005, pp. 3809 – 3813.

[12] R. Stewart and C. Metz, "SCTP: New transport protocol for TCP/IP," *IEEE Internet Computing*, vol. 5, no. 6, pp. 64–69, November/December 2001.

[13] T.V. Lakshman and U. Madhow, "The performance of TCP/IP for networks with high bandwidth-delay products and random loss," *IEEE/ACM Transactions on Networking*, vol. 5, no. 3, pp. 336–350, June 1997.

[14] M. Mathis, J. Semke, and J. Mahdavi, "The macroscopic behavior of the TCP congestion avoidance algorithm," *Computer Communications Review*, vol. 27, no. 3, pp. 67–82, July 1997.

[15] J. Padhye, V. Firoiu, D.F. Towsley, and J.F. Kurose, "Modeling TCP Reno performance: a simple model and its empirical validation," *IEEE/ACM Transactions on Networking*, vol. 8, no. 2, pp. 133–145, April 2000.

[16] C. Casetti and M. Meo, "A new approach to model the stationary behavior of TCP connections," in *IEEE INFOCOM 2000*, Tel-Aviv, Israel, March 2000, pp. 367–375.

[17] C. Casetti and M. Meo, "Modeling the stationary behavior of TCP Reno connections," in *International Workshop on Quality of Service in Multiservice IP Networks*, Rome, Italy, January 2001, pp. 141 – 156.

[18] Takayuki Osogami Adam Wierman and Jorgen Olsn, "A unified framework for modeling TCP-Vegas, TCP-SACK, and TCP-Reno," in *11th IEEE/ACM International Symposium on Modeling, Analysis and Simulation of Computer Telecommunications Systems*, Orlando, Florida, Octobor 2003, pp. 269–278.

[19] R. Stewart and Q. Xie et. al., "Stream control transmission protocol," IETF RFC 2960, October 2000.

[20] M.Garetto, R. Cigno, M. Meo, and M.A. Marsan, "Closed queueing network models of interacting long-lived TCP flows," *IEEE/ACM Transactions on Networking*, vol. 12, no. 2, pp. 300–311, April 2004.

[21] T. S. Rappaport, *Wireless Communications: Principles and Practice*, Prentice Hall, Upper Saddle River, NJ, 2nd edition, December 2001.

[22] *The Network Simulator - ns-2*, http://www.isi.edu/nsnam/ns/.